

# R&D on a high-performance electromagnetic calorimeter based on oriented crystalline scintillators

CALOR 2024

Tsukuba  
つくば市

May 21<sup>th</sup>, 2024

**Mattia Soldani**

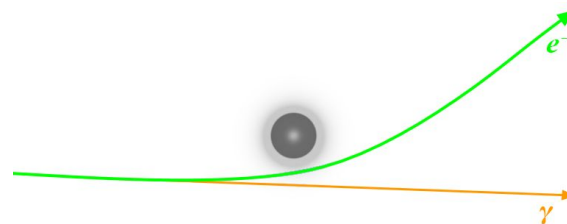
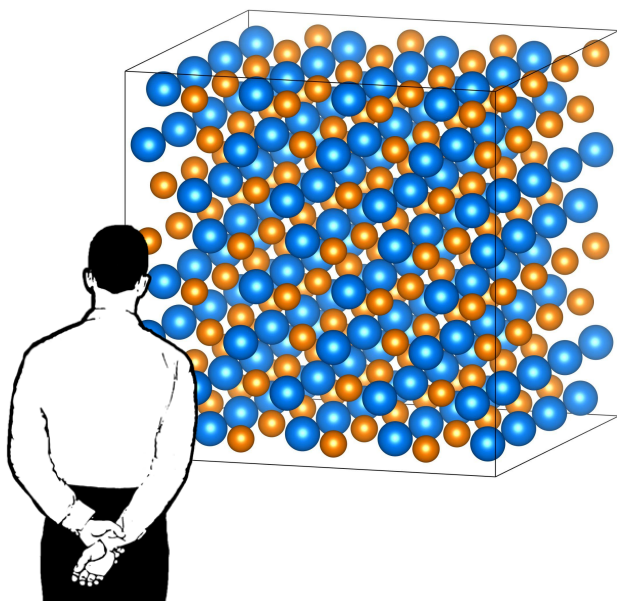
on behalf of the OREO project

[mattia.soldani@Inf.infn.it](mailto:mattia.soldani@Inf.infn.it)

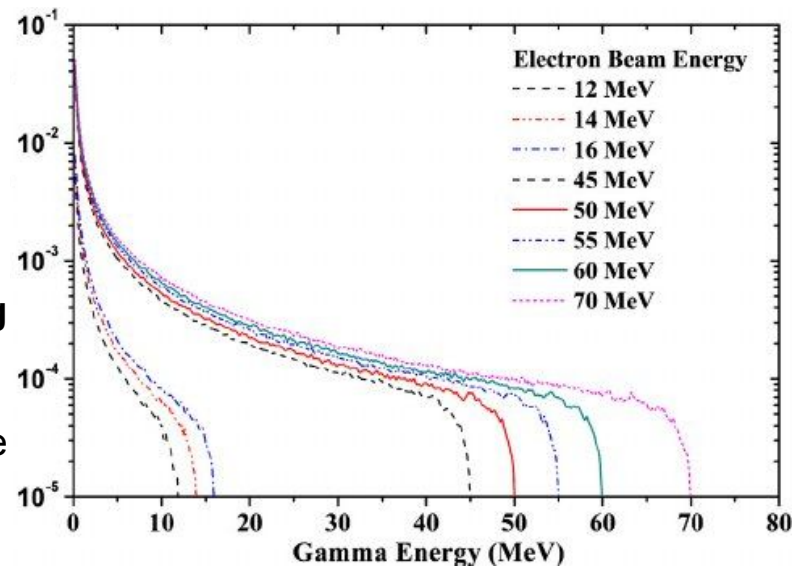
# lattice random orientation

in amorphous media and randomly oriented crystals

electromagnetic interactions occur with one particle at a time, in an incoherent succession of mutually independent events



features of **both bremsstrahlung and pair production** are well-known since [Bethe & Heitler \(1934\)](#)



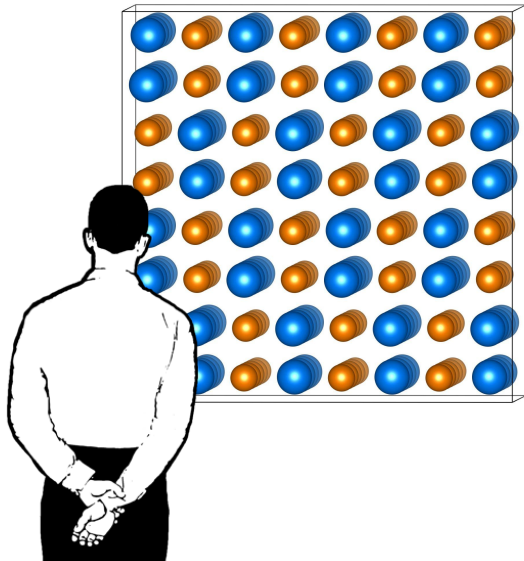
[Naik et al. \(2013\)](#)

## lattice on axis

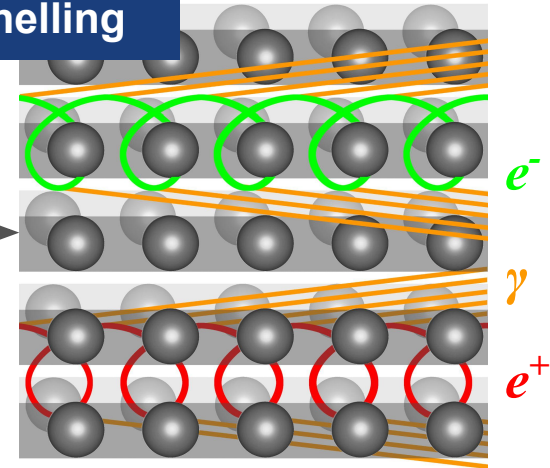
single-atom potentials from the same string sum up coherently  $\Rightarrow$  continuous potential along the direction of the lattice axes

$$\psi_L \xrightarrow{v \rightarrow c} \sqrt{\frac{2U_0}{E_0}} \frac{\text{lattice potential}}{\text{projectile energy}}$$

[Lindhard \(1965\)](#)

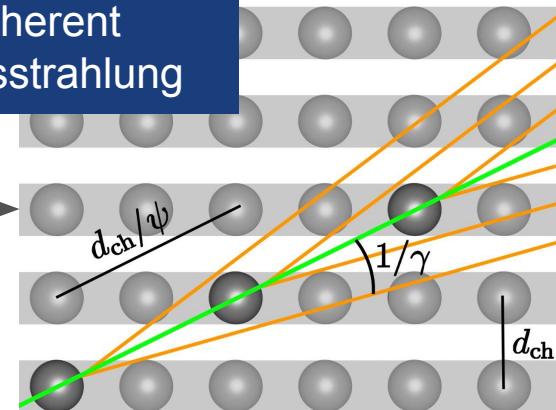


## channelling



## Coherent Bremsstrahlung

out



lattice on axis

energy threshold

- ⇒ ≥ 10-20 GeV in high-Z, high-density crystals
- ⇒ limited effects already for  $\chi \geq 0.1$   
i.e. already at the GeV scale

angular acceptance

- ⇒ independent on the energy and, when above threshold, much larger than  $\psi_L$
- ⇒ ≤ 1 mrad in high-Z, high-density crystals but CB contributes up to  $\sim 1^\circ$

Lorentz boost  $\gamma E$  lattice field in the lab

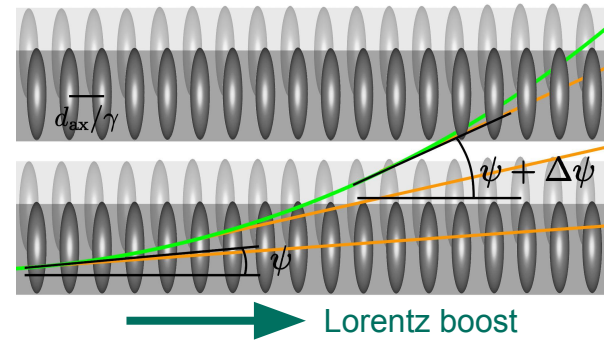
$$\chi = \frac{\gamma E}{E_0} > 1$$

only depends on Nature's constants

$$E_0 = \frac{m^2 c^3}{e \hbar} = 1.32 \cdot 10^{18} \frac{V}{m}$$

lattice potential

$$\Theta_0 < \frac{U_0}{m c^2}$$

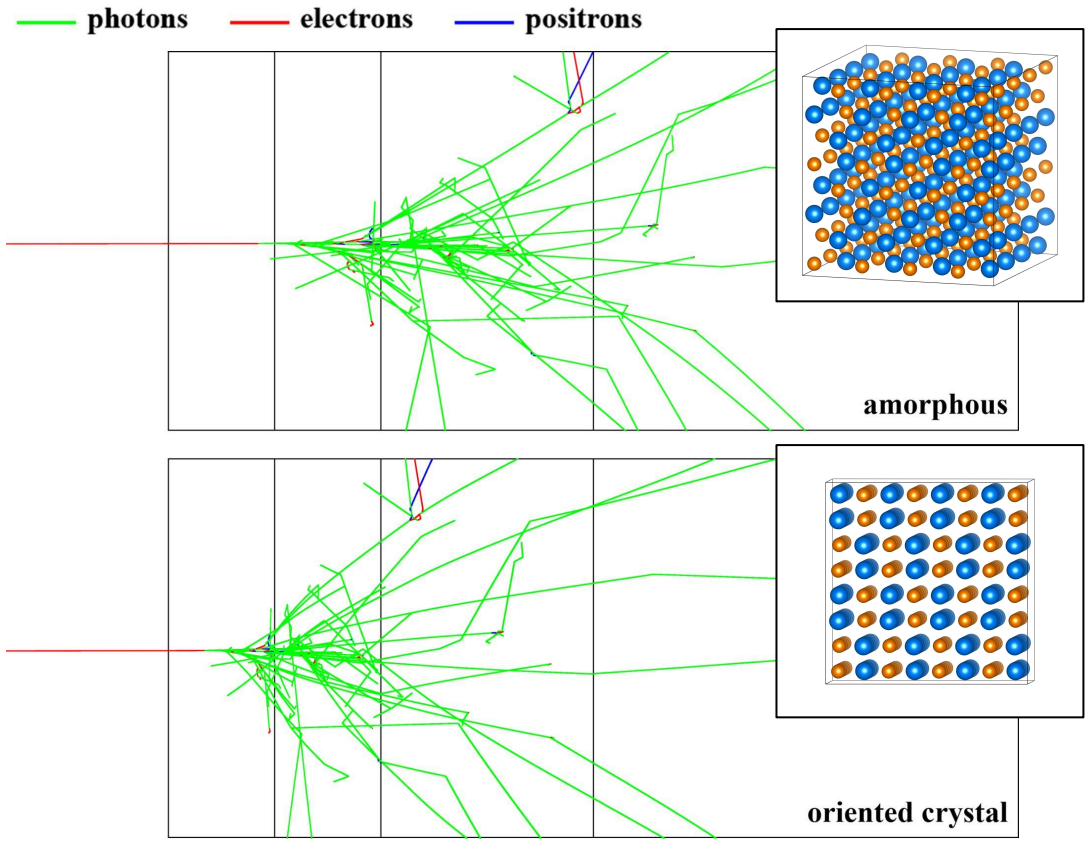


⇒ Strong Field

⇒ enhanced hard photon emission  
(= quantum synchrotron radiation)

⇒ enhanced pair production

# the on-axis em cascade



(not an actual G4 event – for visualisation only)

## overall

electromagnetic shower development is **accelerated**

or equivalently

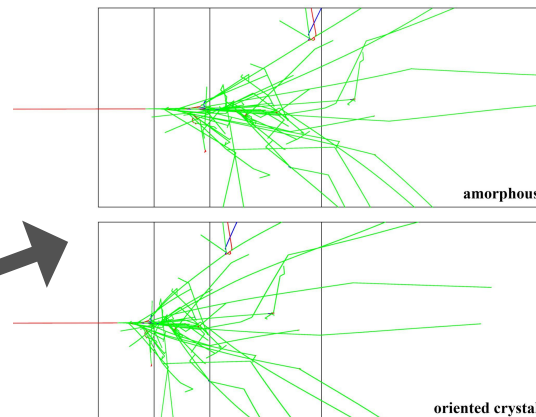
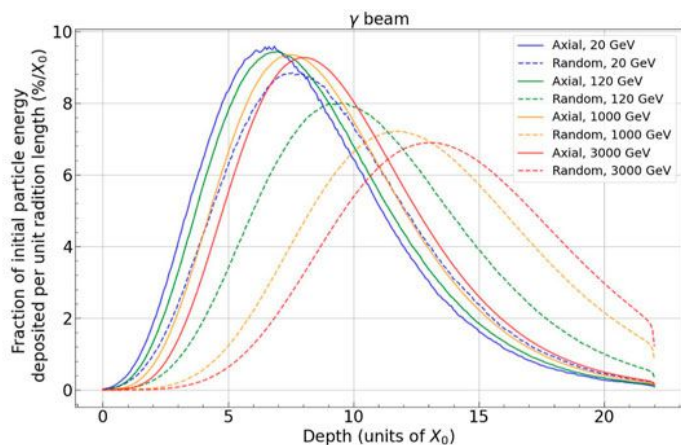
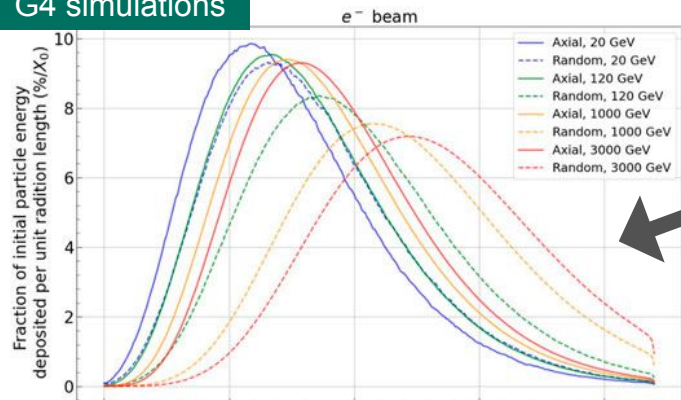
effective radiation length  $X_0$  is **much shorter**

appealing in view of next-generation ECALS

...

# the on-axis em cascade

## G4 simulations



- shower front is shorter due to the SF effects on the primary and early core
- peak is at smaller depth
- peak depth is essentially independent on the primary energy and type
- effect gradually decreases as the shower develops  
 ⇒ shower tail is unaffected by the lattice orientation



# the **OR**ient**Ed** cal**OR**imeter project

## aim

from the full characterisation of lattice-borne effects to the shower development in oriented PWO (lead tungstate)

- simulation models
- measurements with different particles at increasing thickness

to the development and test of an oriented crystal-calorimeter demonstrator

- compactness
- improved energy resolution
- improved particle ID

# PbWO<sub>4</sub> as a scintillator

main light component @ 420 nm  
 ⇒ good match for e.g. NUV SiPMs

original **PWO-I** (as in CMS ECAL):

- quite radiation hard
- rather low relative output 0.3% of NaI
- moderately fast ~10 ns

[Annenkov et al. \(2002\)](#)



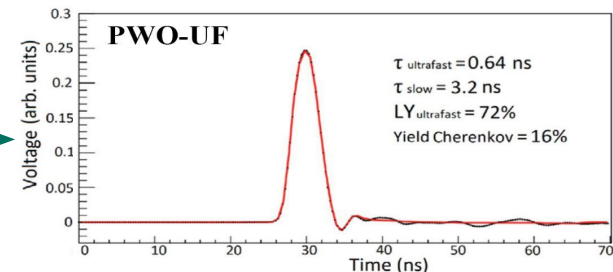
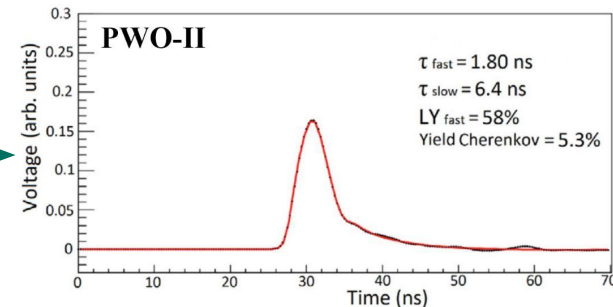
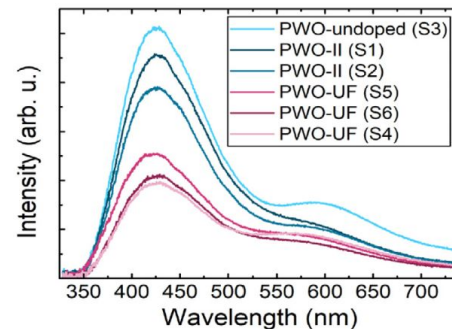
appealing for future detectors...

## PWO-II (for PANDA)

- about same decay time
- ↗ twice the light yield 0.6% of NaI

## PWO-Ultra Fast

- ↘ slightly worse light yield 0.2% of NaI
- ↗ impressive decay time ~640 ps!



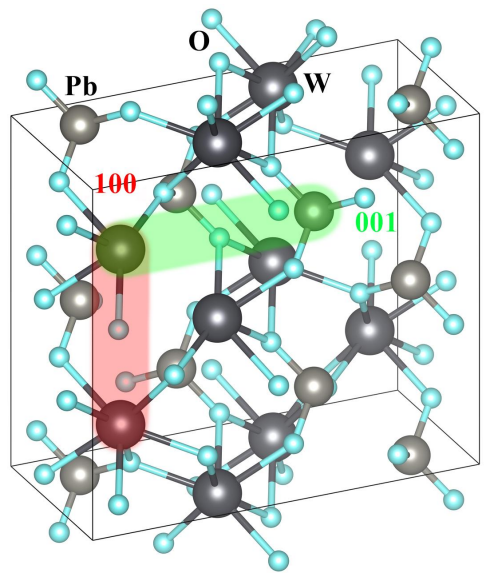
**BRAND NEW!**

in [Korzhiik et al. \(2022\)](#)



# PbWO<sub>4</sub> as a crystal

two of the highest-field axes:

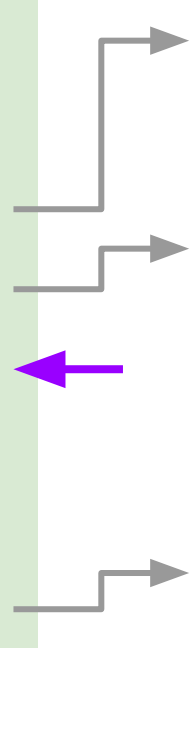


axis	100	001
interatomic pitch [Å]	5.456	12.020
$U_0$ [eV]	464	420
energy threshold [GeV]	23.45	25.90
$\Theta_0$ [mrad]	0.908	0.822
$\Theta_0$ [mrad] @ 5.6 GeV	0.24	0.22
$\Theta_0$ [mrad] @ 120 GeV	5.12	4.63
$\psi_L$ @ 5.6 GeV [mrad]	0.407	0.387
$\psi_L$ @ 120 GeV [mrad]	0.088	0.084

limited SF down to a few GeV

but other coherent effects hold up to  $\sim 1^\circ$

unbound motion: angular acceptance significantly larger than that of channelling (under-barrier)

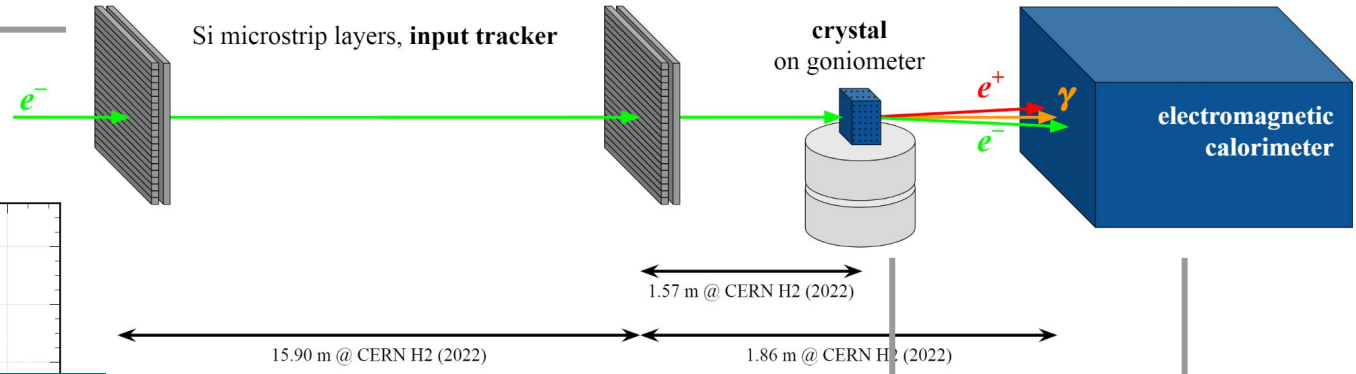
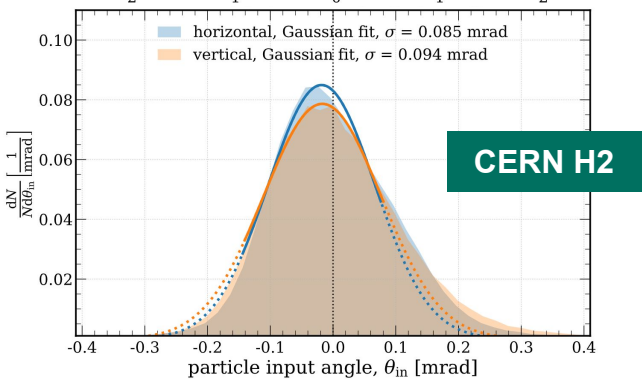
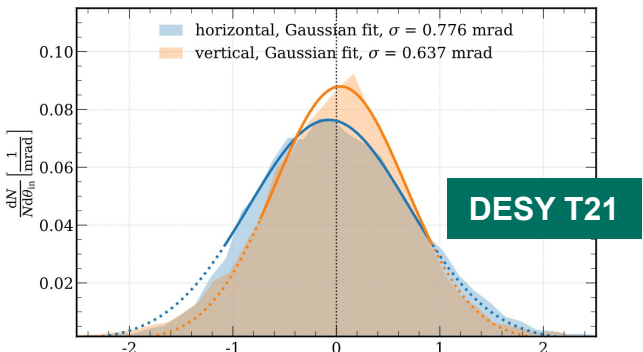


em interactions in oriented PWO

# our measurement campaign

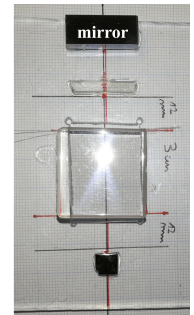
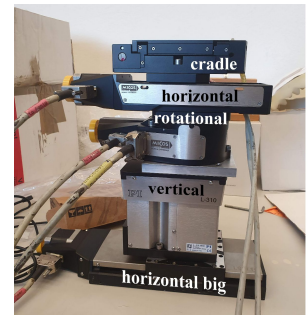
intrinsic resolution between 10-40  $\mu\text{m}$

$\Rightarrow e^-$  beam angles:



angular (transverse axes) stages with precision  $\lesssim 5 \mu\text{rad}$   
 $\Rightarrow$  beam-lattice misalignment angle

lead glass blocks or BGO/PWO arrays



# our measurement campaign

first observation of SF effects to radiation in oriented PWO:  
[Bandiera et al. \(2018\)](#)

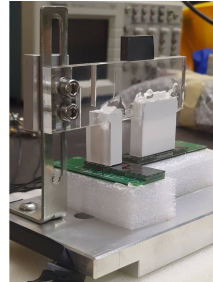
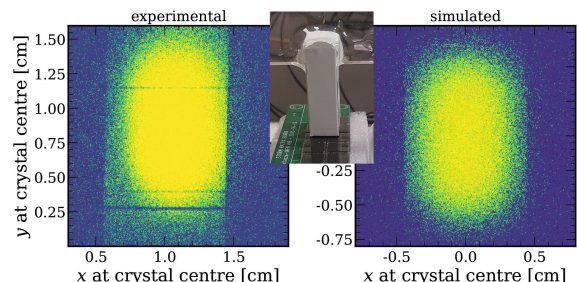
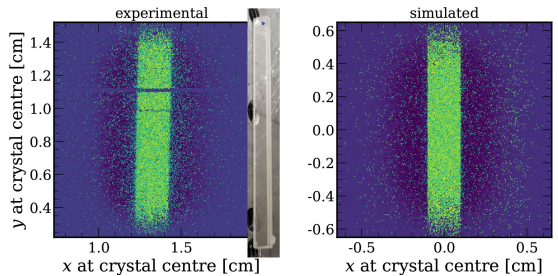
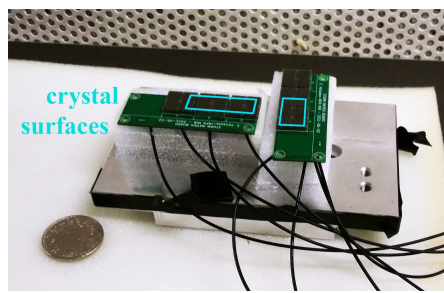
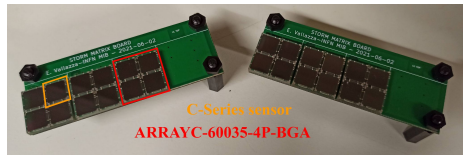
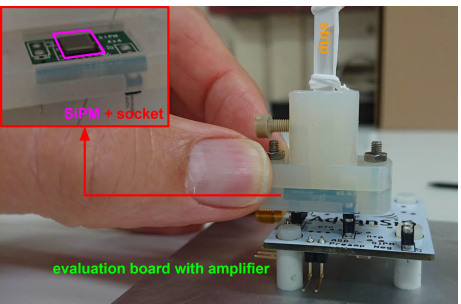
## 2017-19 0.45 X<sub>0</sub> proof of concept

## 2021 1, 2 X<sub>0</sub> getting thicker

- probed with 120 GeV/c e<sup>-</sup> @ CERN SPS H2  
5.6 GeV/c e<sup>-</sup> (no SiPMs) @ DESY T21
- SiPM: AdvanSiD ASD-NUV4S-P [Soldani et al. \(2022\)](#)

- probed with 120 GeV/c e<sup>-</sup> @ CERN SPS H2  
1-100 GeV γ @ CERN SPS H2
- SiPM: [onsemi ARRAYC-60035-4P-BGA](#) arrays

⇒ standardisation  
[Selmi et al. \(2023\)](#)



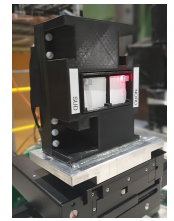
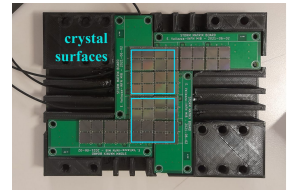
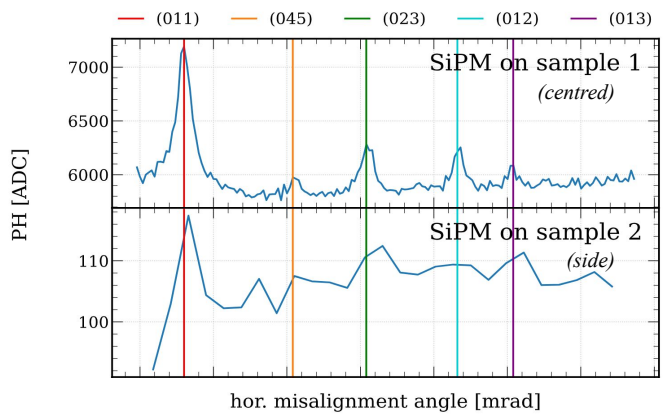
# our measurement campaign

putting everything together:  
[Soldani et al. \(2024\)](#)

## 2022

4.6 X<sub>0</sub> THICKER

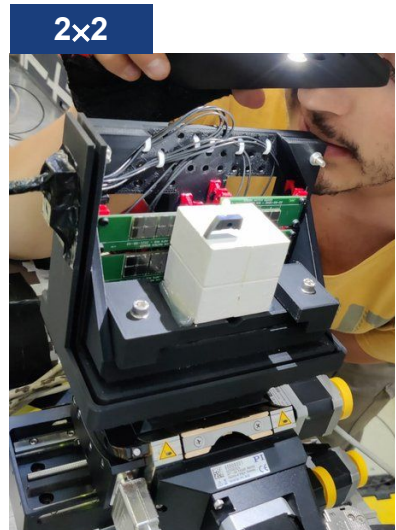
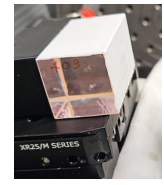
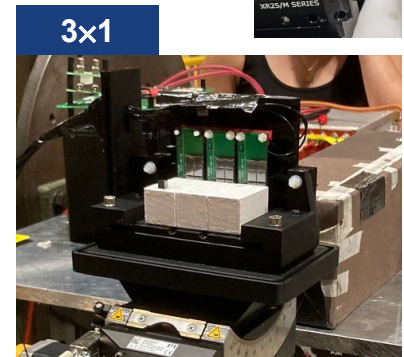
- probed with 100, 120 GeV/c e<sup>-</sup> @ CERN SPS H2
- SiPM: [onsemi ARRAYC-60035-4P-BGA](#) arrays on the back
- preliminary test of (purely mechanical) mutual alignment between 2 identical samples and shower sharing



## 2023

5 X<sub>0</sub> arrays time to go multi-cell

- probed with 5-15 GeV/c e<sup>-</sup> @ CERN PS T9  
 40-150 GeV γ @ CERN SPS H2
- SiPM: [onsemi ARRAYC-60035-4P-BGA](#) arrays
- cells glued to one another and optically isolated

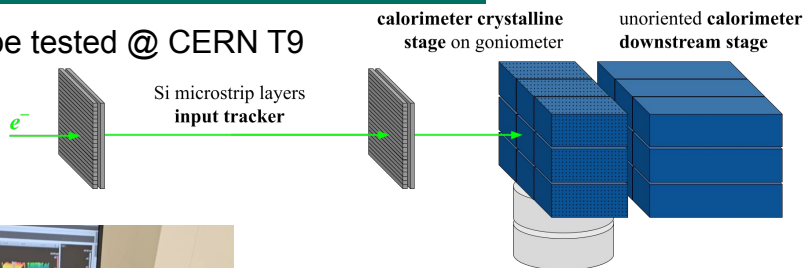


# towards a fine-segmentation ECAL

## 2024-25

### the OREO prototype

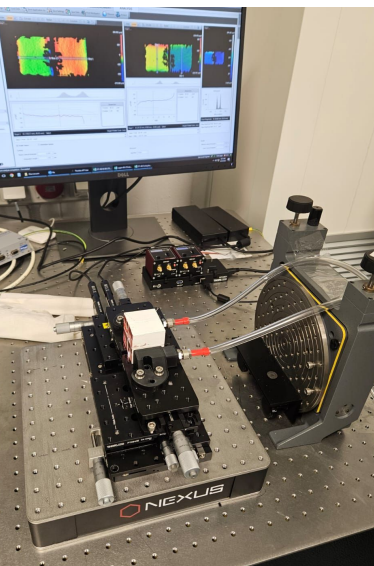
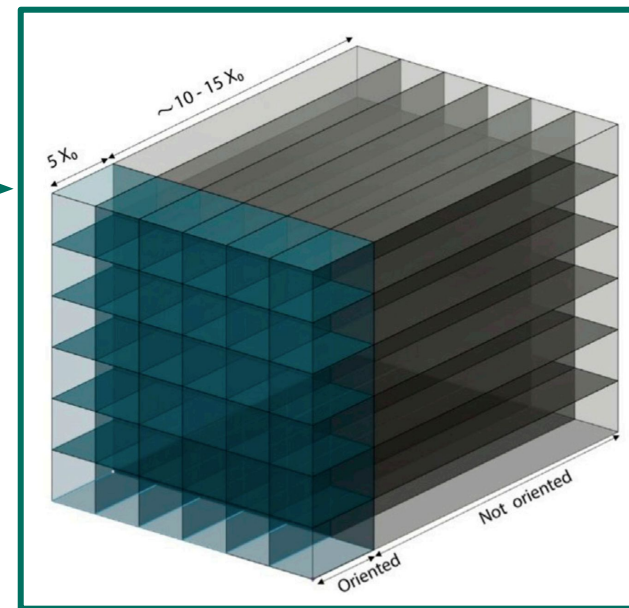
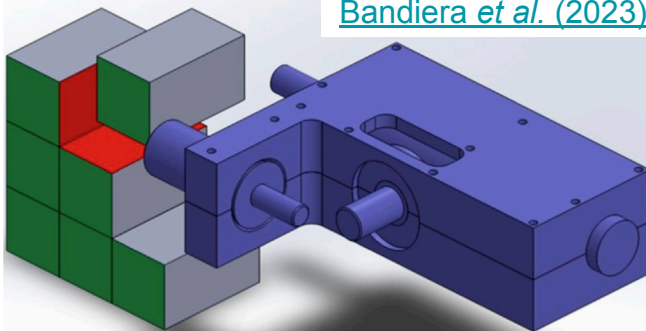
to be tested @ CERN T9



3x3 oriented layer  $\sim 5 X_0$   
and 3x3 unoriented layer  $\gg 5 X_0$

surface (not axis) non-projective geometry

[Bandiera et al. \(2023\)](#)



crystals mutually aligned within  $\sim \Theta_0/2$  maximum

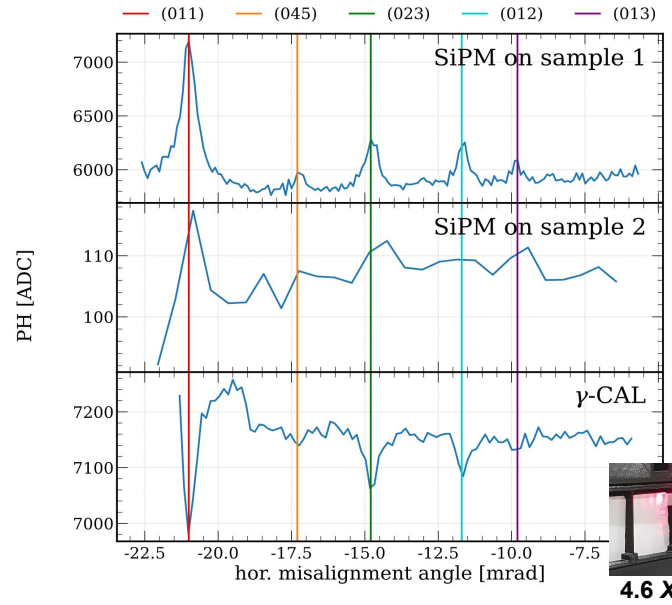
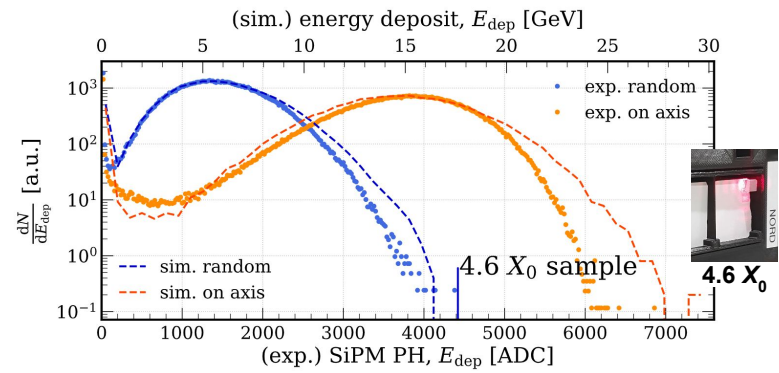
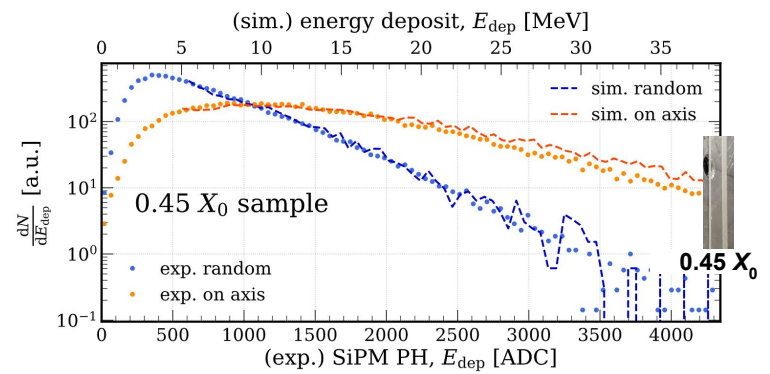
### gluing procedure

- preliminary lattice characterisation with laser autocollimator and HRXR
- on roto-translational adjusters  $\rightarrow$  real-time corrections of relative miscut
- Fizeau interferometry for real-time check

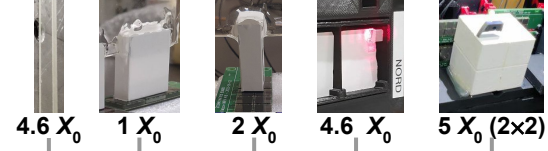
a selection of our results

# LY enhancement

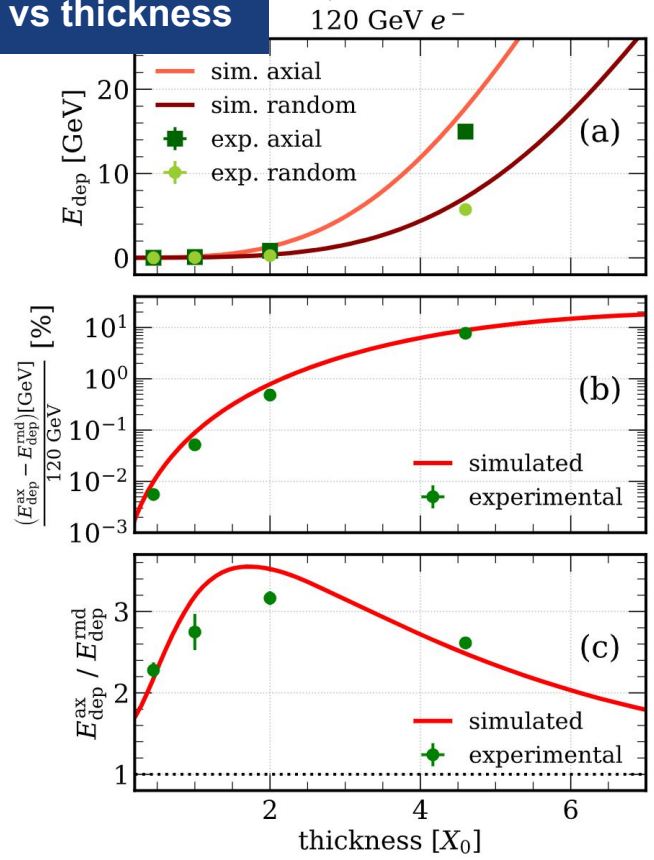
- light output is highly sensitive to the lattice effects
  - not only the strong axes, also higher-order planes
  - light spectrum modification even at  $< X_0$
- excellent agreement with G4 simulations (energy deposit)



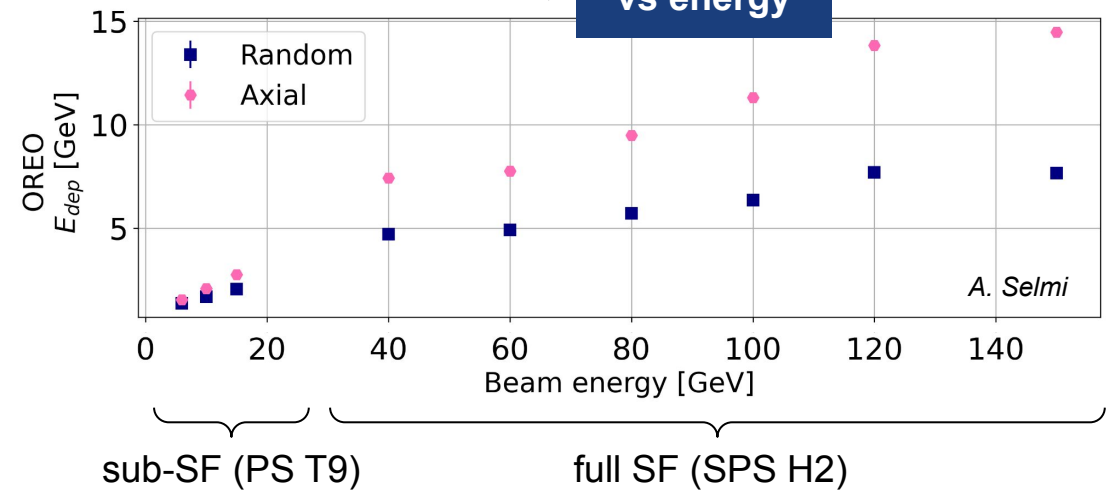
# em interactions in oriented PWO shower acceleration



## vs thickness



## vs energy

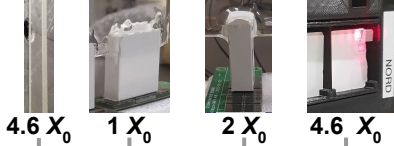


## with electrons

- on-axis energy deposit curve is steeper → shower is accelerated
- axis-random fractional energy deposit difference spans over 4 orders of magnitude!
- axis-random enhancement
  - is peaked at  $\sim 1.5 X_0$  at 120 GeV/c
  - grows with the incident electron energy

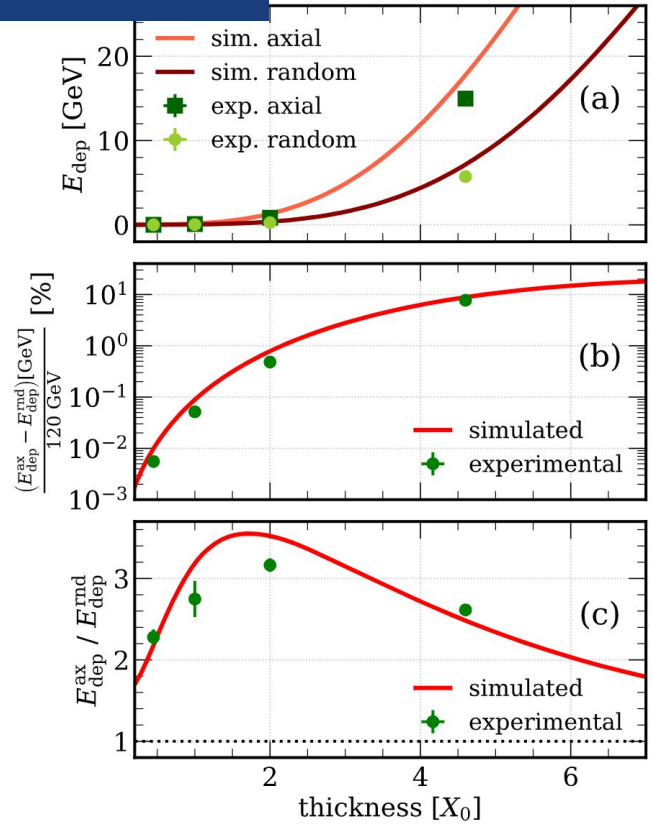


# em interactions in oriented PWO shower acceleration



vs thickness

120 GeV  $e^-$

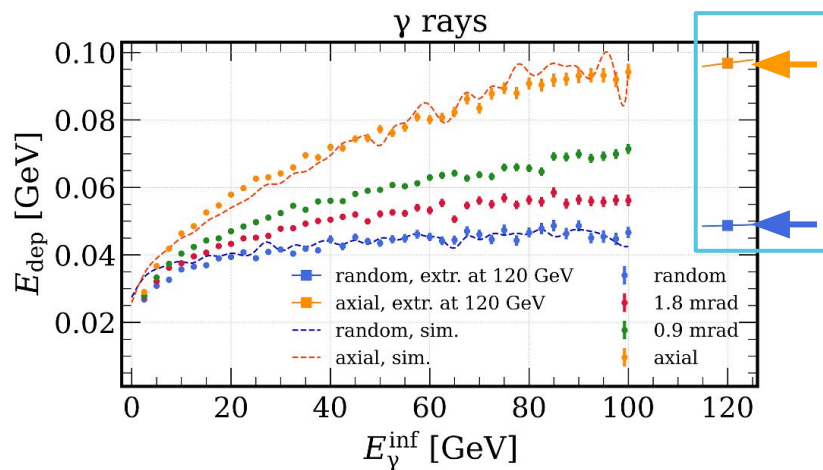
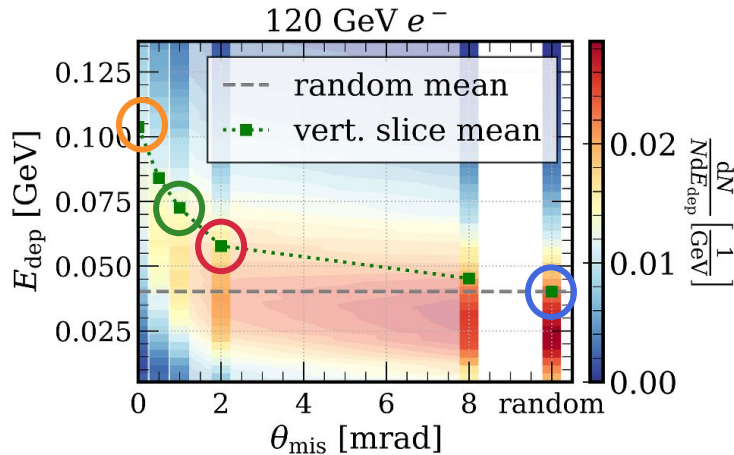


thickness $[X_0]$	effective thickness $[X_0]$	thickness enhancement [%]
0.45	0.745	165.48
1	1.520	151.98
2	2.923	146.17
4.6	6.208	134.96

reduction of the effective  $X_0$ !

em interactions in oriented PWO

## electrons vs photons



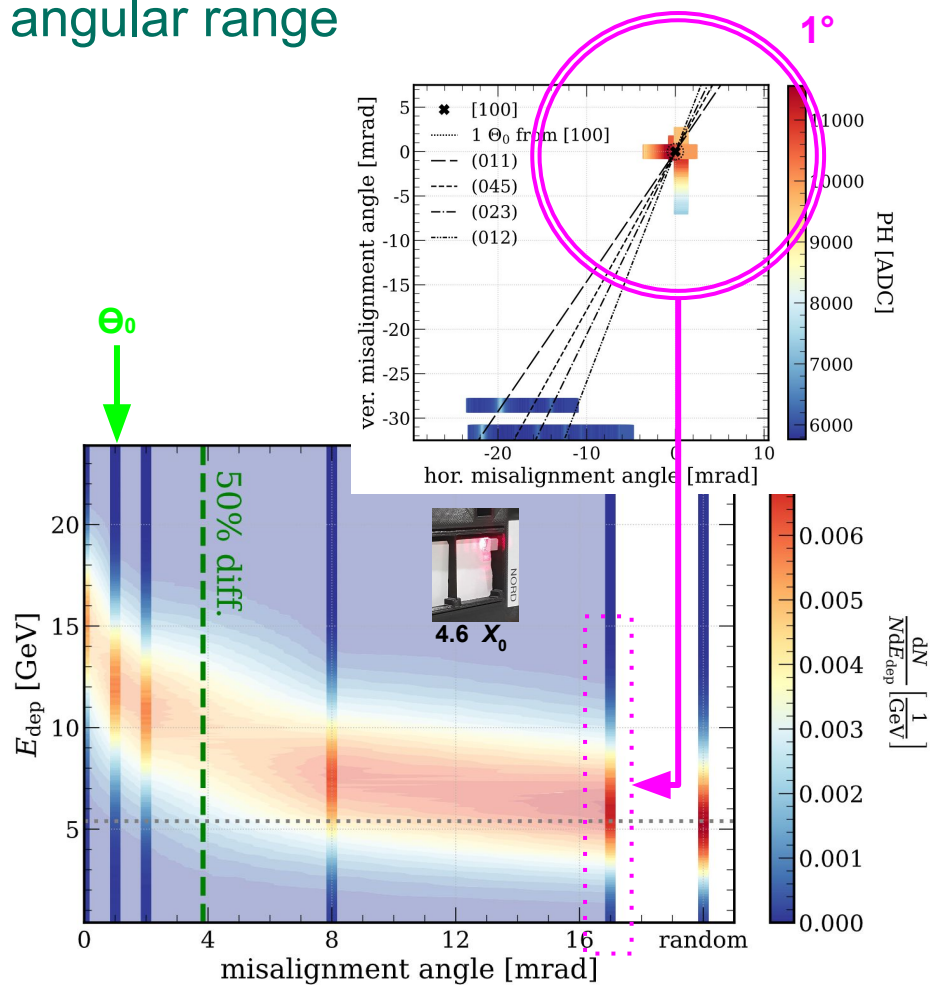
- data with bremsstrahlung photons between 1 and 10 GeV
- extrapolation to 120 GeV

$$a \cdot \log(bE_{\gamma} - c)$$

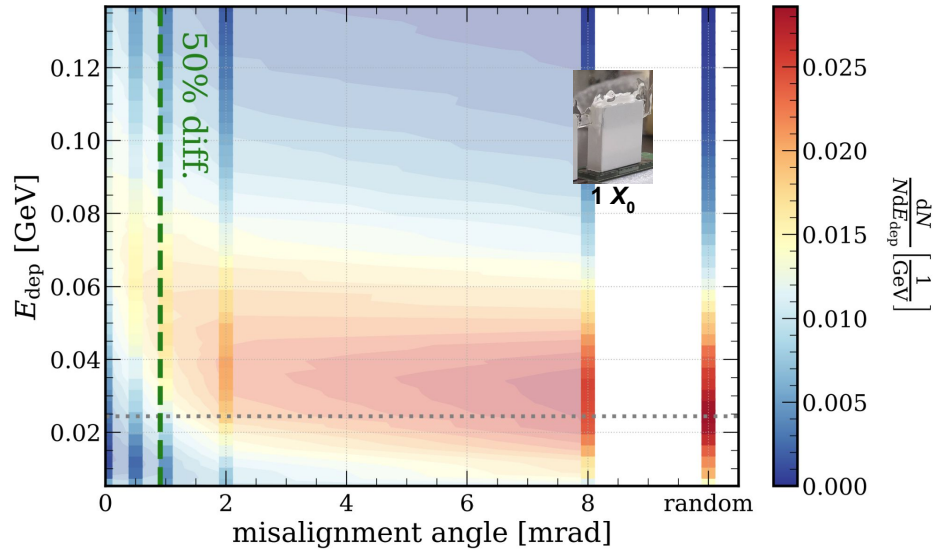
→ consistent with the data collected with 120 GeV/c electrons at different misalignment angles

(accounting for the  $e^{\pm}/\gamma$  development difference)

em interactions in oriented PWO  
angular range



- enhancement is angle-dependent
  - sharp peak at  $\lesssim \Theta_0 \sim 1$  mrad
  - still different from random at  $\sim 1^\circ$
- width is sample dependent
  - depends on sample mosaicity
  - shower develops more in thicker samples  $\Rightarrow$  more lower-energy secondaries, within range of channelling ( $\psi_L$ ) and CB ( $\sim 10\psi_L$ )



# em interactions in oriented PWO vs hadronic interactions

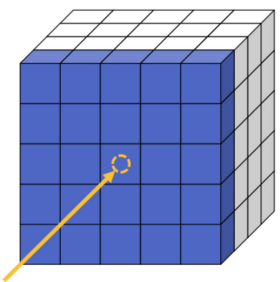
$X_0$  (em) is reduced, whereas  $\lambda_{int}$  (hadronic) is unaffected  $\Rightarrow$   $\gamma$ /hadron discrimination

PRELIMINARY measurements

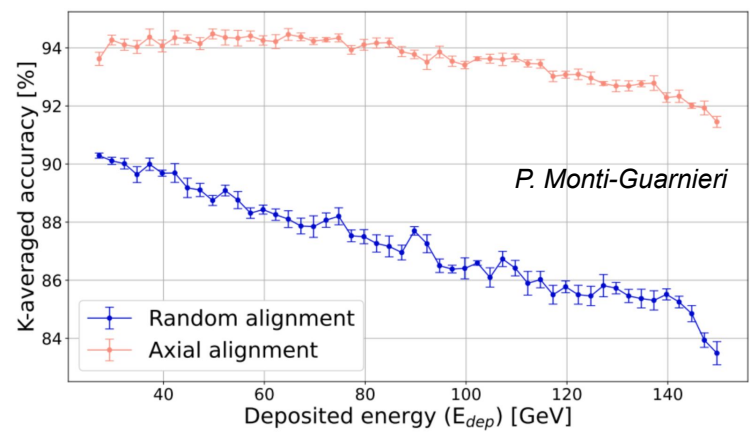
G4 simulation studies

$\gamma$ /n populations with initial energy 26-151 GeV in a highly segmented PWO full calorimeter:

5x5x4 crystals of size 1x1x4 cm<sup>3</sup>

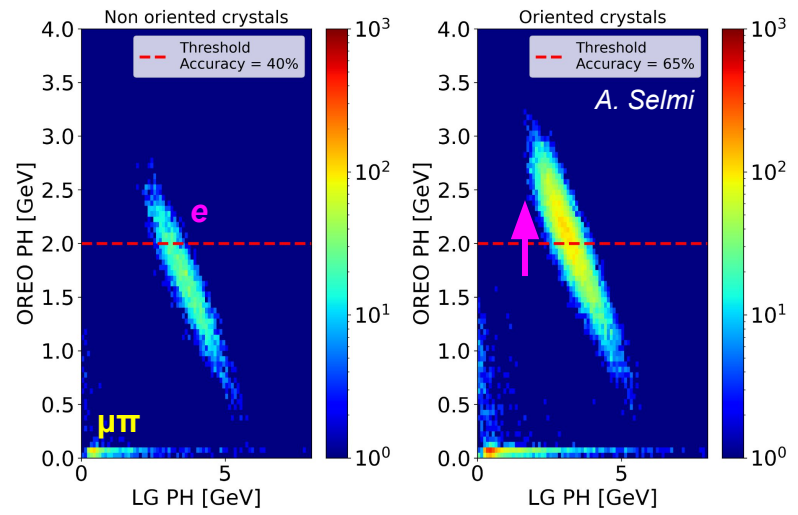


random forest classification



PWO preshower on goniometer in front of Pb glass block

5 X<sub>0</sub> (2x2)



# exciting times ahead!

several progress throughout the years in

- probing crystalline SF effects
- developing sound simulation tools + integration with Geant4
- designing an operational longitudinally segmented, oriented-calorimeter prototype

getting ready for integration in

**keep track of the lattice orientation** to avoid uncontrolled lattice effects when building a crystal calorimeter!

## space-borne $\gamma$ -ray (VHE/UHE) detectors with pointing systems

à la Fermi LAT

- reduced thickness  $\Rightarrow$  more payload available for transverse size increase  $\Rightarrow$  acceptance
- improved shower containment  $\Rightarrow$  less longitudinal leakage
- higher  $\gamma$  efficiency
- better  $\gamma$ /hadron discrimination

see e.g. [Bandiera et al. \(2023\)](#), [Gaitskell et al. \(2023\)](#)

## forward-geometry accelerator-based experiments

fixed-target    collider forward region

- improved shower containment  $\Rightarrow$  energy resolution
- higher  $\gamma$  efficiency  $\Rightarrow$  ideal for  $\gamma$  vetoes
- better  $\gamma$ /hadron discrimination  $\Rightarrow$  ideal for  $\gamma$ /n in small-angle calorimeters on neutral hadron beamlines e.g. HIKE [CERN-SPSC-2022-031](#)



thank you!    どうもありがとう!

any comments or questions? contact me at [mattia.soldani@Inf.infn.it](mailto:mattia.soldani@Inf.infn.it)!

supplemental material

N. Argiolas<sup>a,b</sup>, L. Bandiera<sup>c</sup>, V. Baryshevsky<sup>d</sup>, L. Bomben<sup>e,f</sup>, C. Brizzolari<sup>e,f</sup>, N. Canale<sup>c</sup>,  
S. Carsi<sup>e,f</sup>, S. Cutini<sup>g</sup>, F. Davi<sup>h,c</sup>, D. De Salvador<sup>a,b</sup>, A. Gianoli<sup>c</sup>, V. Guidi<sup>i</sup>,  
V. Haurylavets<sup>d</sup>, M. Korjik<sup>d</sup>, G. Lezzani<sup>e,f</sup>, A. Lobko<sup>d</sup>, F. Longo<sup>j,k</sup>, L. Malagutti<sup>c</sup>,  
S. Mangiacavalli<sup>e,f</sup>, V. Mascagna<sup>e,f</sup>, A. Mazzolari<sup>c,i</sup>, L. Montalto<sup>h</sup>, P. Monti-Guarnieri<sup>c,i,\*\*</sup>,  
M. Moulson<sup>l</sup>, R. Negrello<sup>c,i</sup>, G. Paternò<sup>c</sup>, L. Perna<sup>e,f</sup>, C. Petroselli<sup>e,f</sup>, M. Prest<sup>e,f</sup>,  
D. Rinaldi<sup>h,l</sup>, M. Romagnoni<sup>c,i</sup>, F. Ronchetti<sup>e,f,\*</sup>, G. Saibene<sup>e,f</sup>, A. Selmi<sup>e,f</sup>, F. Sgarbossa<sup>a,b</sup>,  
M. Soldani<sup>l</sup>, A. Sytov<sup>c</sup>, V. Tikhomirov<sup>d</sup>, E. Vallazza<sup>f</sup>

<sup>a</sup>Università degli Studi di Padova, Padua, Italy

<sup>b</sup>INFN Laboratori Nazionali di Legnaro, Legnaro, Italy

<sup>c</sup>INFN Sezione di Ferrara, Ferrara, Italy

<sup>d</sup>Institute for Nuclear Problems, Belarusian State University, Minsk, Belarus

<sup>e</sup>Università degli Studi dell'Insubria, Como, Italy

<sup>f</sup>INFN Sezione di Milano Bicocca, Milan, Italy

<sup>g</sup>INFN Sezione di Perugia, Perugia, Italy

<sup>h</sup>Università Politecnica delle Marche, Ancona, Italy

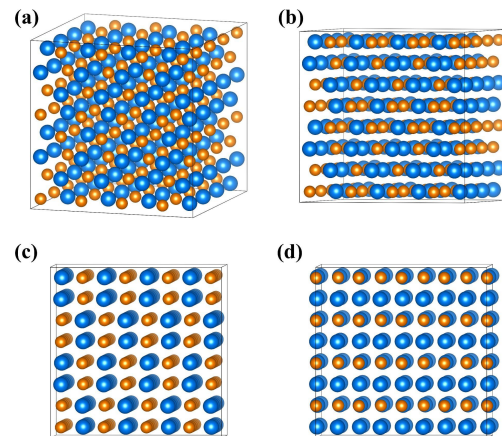
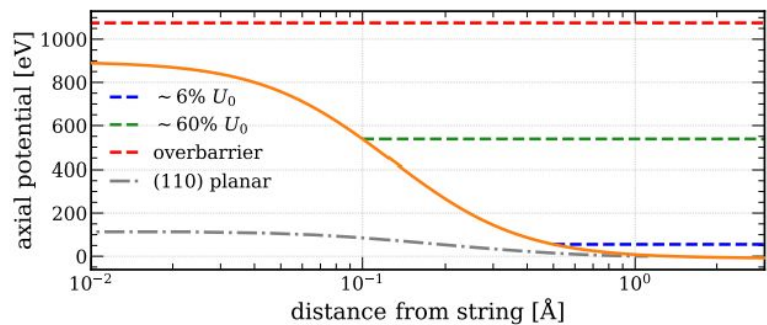
<sup>i</sup>Università degli Studi di Ferrara, Ferrara, Italy

<sup>j</sup>Università degli Studi di Trieste, Trieste, Italy

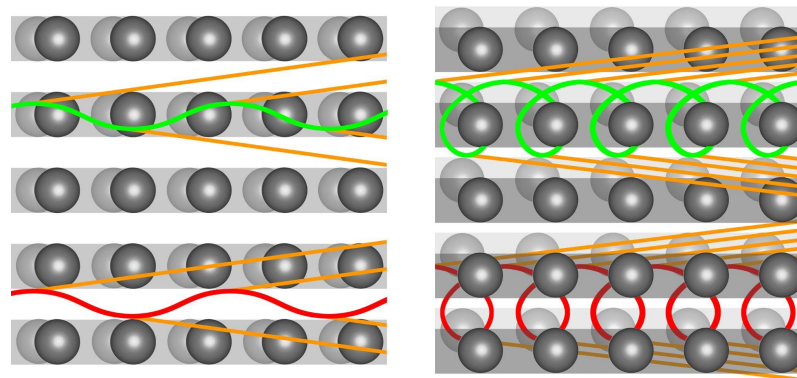
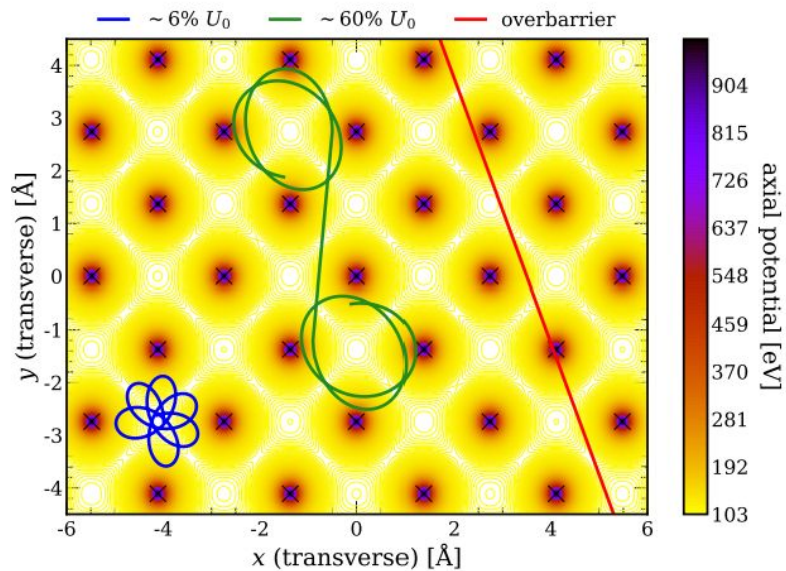
<sup>k</sup>INFN Sezione di Trieste, Trieste, Italy



## planes vs axes



- a) amorphous
- b) planar
- c) axial, [100]-like
- d) axial, [001]-like



# scintillating media

## inorganic (crystals)

- ↗ high-Z → homogeneous calorimeters
- ↘ typically slow  $> \text{ns}$ , up to  $\mu\text{s}$   
& tradeoff between LY and timing
- ↘ many technological challenges  
(growth, machining, support...)
- ↘ expensive
- ↘ LY depends on temperature  $O(\%/^{\circ}\text{C})$

## organic (plastic)

- ↘ low density and Z
  - ↗ fast response  $\lesssim \text{ns}$
  - ↗ easy to handle and scale
  - ↗ comparatively easier to craft
  - ↗ comparatively cheaper
- ⇒ ideal active medium in sampling calorimeters

# (common) inorganic scintillators

Parameter:	$\rho$	MP	$X_0^*$	$R_M^*$	$dE^*/dx$	$\lambda_I^*$	$\tau_{\text{decay}}$	$\lambda_{\text{max}}$	$n^{\ddagger}$	Relative output <sup>†</sup>	Hygroscopic?	$d(\text{LY})/dT$
Units:	$\text{g/cm}^3$	$^\circ\text{C}$	cm	cm	MeV/cm	cm	ns	nm				$\%/^\circ\text{C}^{\ddagger}$
NaI(Tl)	3.67	651	2.59	4.13	4.8	42.9	245	410	1.85	100	yes	-0.2
BGO	7.13	1050	1.12	2.23	9.0	22.8	300	480	2.15	21	no	-0.9
BaF <sub>2</sub>	4.89	1280	2.03	3.10	6.5	30.7	650 <sup>s</sup>	300 <sup>s</sup>	1.50	36 <sup>s</sup>	no	-1.9 <sup>s</sup>
							0.9 <sup>f</sup>	220 <sup>f</sup>		4.1 <sup>f</sup>		0.1 <sup>f</sup>
CsI(Tl)	4.51	621	1.86	3.57	5.6	39.3	1220	550	1.79	165	slight	0.4
CsI(Na)	4.51	621	1.86	3.57	5.6	39.3	690	420	1.84	88	yes	0.4
CsI(pure)	4.51	621	1.86	3.57	5.6	39.3	30 <sup>s</sup>	310	1.95	3.6 <sup>s</sup>	slight	-1.4
							6 <sup>f</sup>			1.1 <sup>f</sup>		
PbWO <sub>4</sub>	8.30	1123	0.89	2.00	10.1	20.7	30 <sup>s</sup>	425 <sup>s</sup>	2.20	0.3 <sup>s</sup>	no	-2.5
							10 <sup>f</sup>	420 <sup>f</sup>		0.077 <sup>f</sup>		
LSO(Ce)	7.40	2050	1.14	2.07	9.6	20.9	40	402	1.82	85	no	-0.2
PbF <sub>2</sub>	7.77	824	0.93	2.21	9.4	21.0	-	-	-	Cherenkov	no	-
CeF <sub>3</sub>	6.16	1460	1.70	2.41	8.42	23.2	30	340	1.62	7.3	no	0
LaBr <sub>3</sub> (Ce)	5.29	783	1.88	2.85	6.90	30.4	20	356	1.9	180	yes	0.2
CeBr <sub>3</sub>	5.23	722	1.96	2.97	6.65	31.5	17	371	1.9	165	yes	-0.1

\* Numerical values calculated using formulae in this review.

<sup>‡</sup> Refractive index at the wavelength of the emission maximum.

<sup>†</sup> Relative light output measured for samples of 1.5  $X_0$  cube with a Tyvek paper wrapping and a full end face coupled to a photodetector. The quantum efficiencies of the photodetector are taken out.

<sup>‡</sup> Variation of light yield with temperature evaluated at the room temperature.

*f* = fast component, *s* = slow component

# more on PWO and its generations





$Z/A$	0.41315
$\rho$ [g/cm <sup>3</sup> ]	8.3
Standard $X_0$ [mm]	8.903
Standard $R_M$ [mm]	19.59
$E_C$ for $e^-$ [MeV]	9.64
$E_C$ for $e^+$ [MeV]	9.31
Nuclear collision length [mm]	121.2
Nuclear interaction length [mm]	202.7
Pion collision length [mm]	152.1
Pion interaction length [mm]	240.4

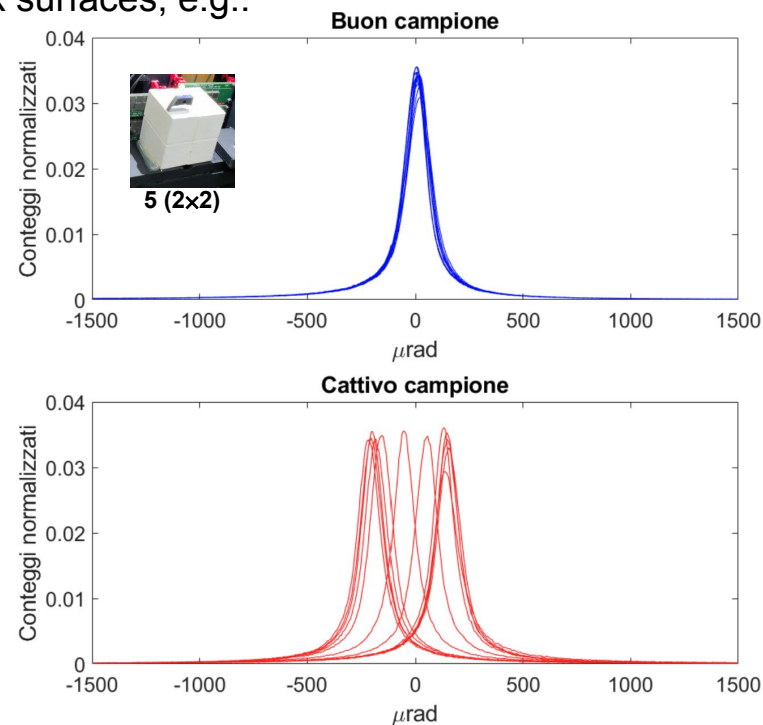
	PWO-I	PWO-II	PWO-UF
$\rho$ [g/cm <sup>3</sup> ]	8.28 [30]	8.28 [198]	8.27 [201]
Scintillation max. [nm]	420 [30]	420 [198]	420 [201]
LY [ph. $e^-$ /MeV]	8–12 [205]	17–22 [205]	7 [201]
LY rel. to NaI [%]	0.3 [30]	0.6 [198]	about 0.2
$\tau_{\text{decay}}$ [ns]	10–30 [30, 205] 6.5 [198]	10–30 [30, 205] 6.5 [198]	0.64 [201]
$-dLY/dT$ [%/°C]	2.5 [30]	3 [205]	about 0.4 [201]
dk [1/m]	1.5 [205]	1 [205]	0.3 [201]

see [Soldani, PhD thesis \(2023\)](#) and references therein

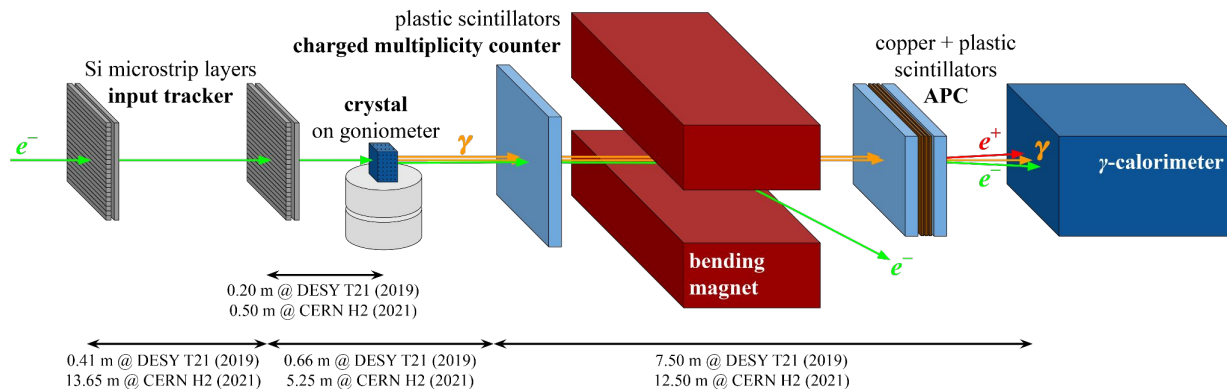
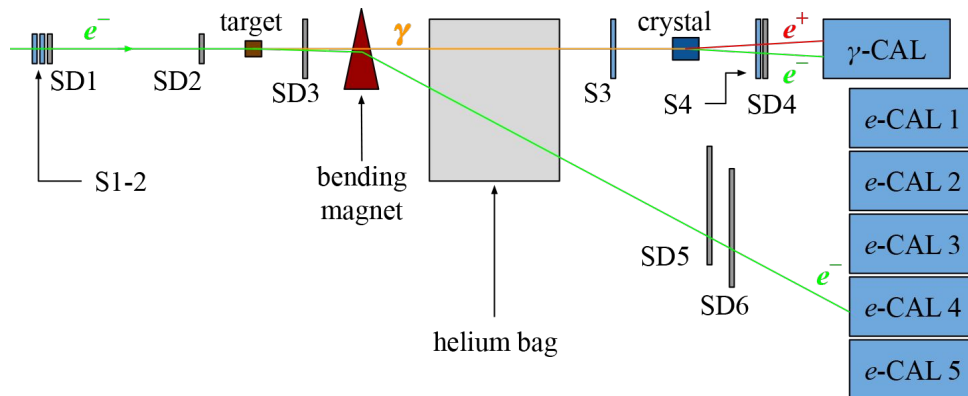
## our PWO samples

characterisation w/ HRXRD scanning  
the sample front/back surfaces, e.g.:

				
Thickness [ $X_0$ ]	<b>0.45</b>	<b>1</b>	<b>2</b>	<b>4.6</b>
Thickness [mm]	4	9	18	41
Transv. size [mm <sup>2</sup> ]	2 × 55	~ 30 × 30	9 × 27	~ 30 × 30
Axis	001	100	001	100
Generation	I	II	I	I
Surface mosaicity [ $\mu$ rad]	~ 100	~ 250	~ 350 (hor.) ~ 550 (ver.)	~ 250
Tested on CERN H2/H4	2016-2018	2021	2021	2022
Tested on DESY T21	2019	2019	no	no



## other beamtest setups

 $e^-$  $\gamma$ 

# beamtest setup

## input tracking modules

$\approx 2 \times 2 \text{ cm}^2$   $xy$  double-sided Si microstrip sensors, with  $50 \text{ }\mu\text{m}$  readout pitch, analog readout and an overall  $\approx 10 \text{ }\mu\text{m}$  single-hit resolution

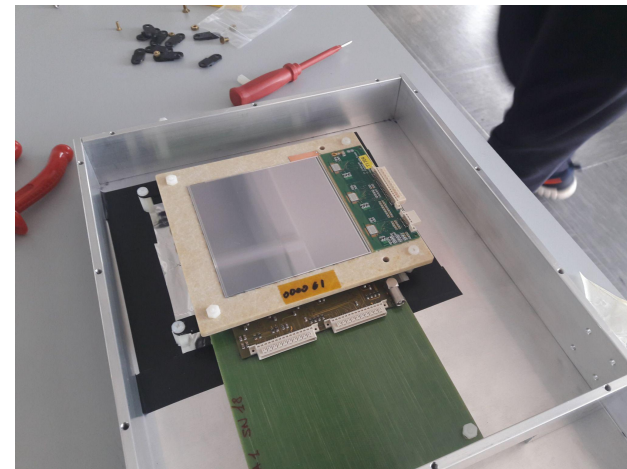
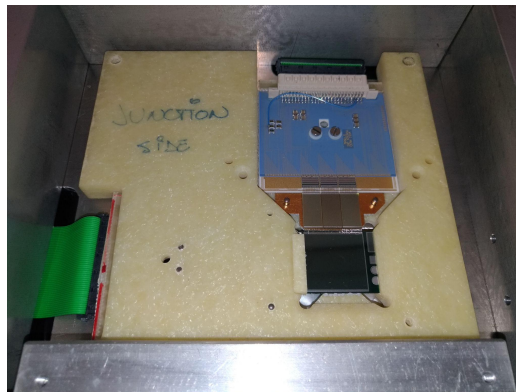
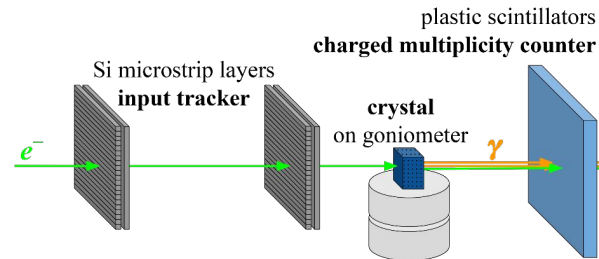
pairs of  $\approx 10 \times 10 \text{ cm}^2$  single-sided Si microstrip sensors, with  $242 \text{ }\mu\text{m}$  readout pitch, analog readout and an overall  $\approx 35 \text{ }\mu\text{m}$  single-hit resolution

## output charged multiplicity counter

one or more  $\approx 10 \times 10 \text{ cm}^2$  plastic scintillator pads read out by PMTs

## goniometer

fine-grained, remote-controlled movements along  $x$ ,  $y$ ,  $\theta_x$  and  $\theta_y$  with  $\approx 5 \text{ }\mu\text{m}/\mu\text{rad}$  resolution

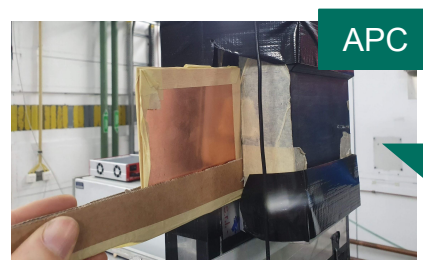
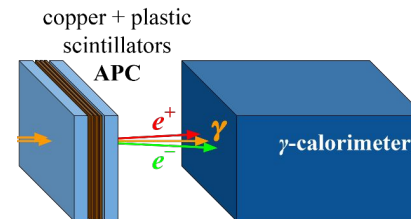


# beamtest setup

different **calorimeters** along the years:

- Stefi: 3×3 matrix of PWO blocks from the CMS endcap, SiPM-based readout
- Genni: 3×3 matrix of BGO blocks from the PADME calorimeter, PMT-based readout
- (OPAL) Pb glass blocks read out by PMTs

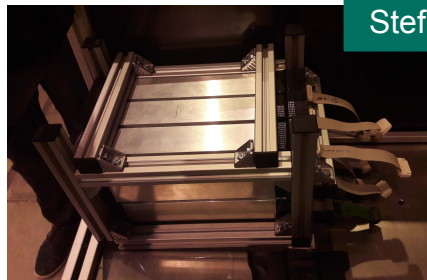
the **Active Photon Converter** was installed and tested for the first time during the 2019 beamtest at DESY T21 → scintillating pads and a Cu converter layer, statistical information on the output photon number distribution



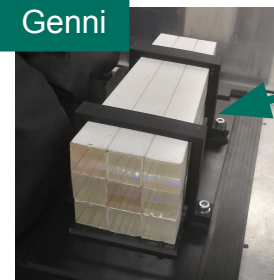
Pb glass



Stefi



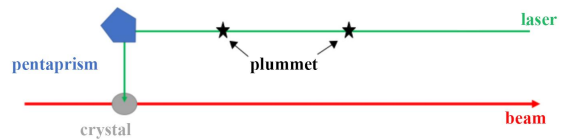
Genni





# sample (pre-)alignment

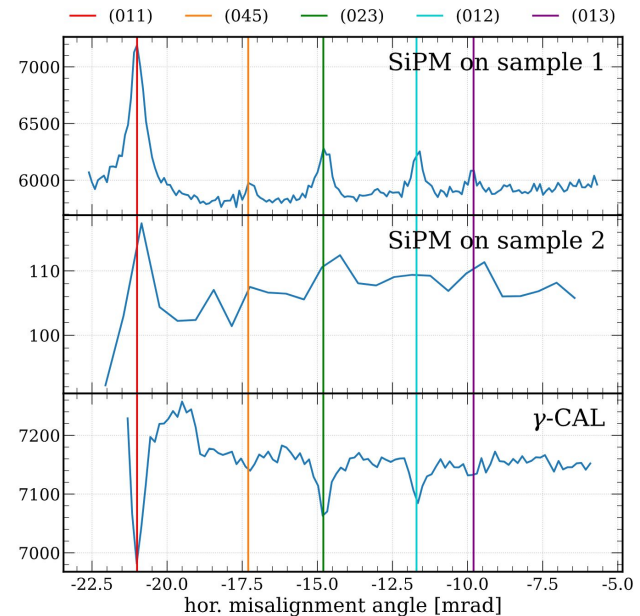
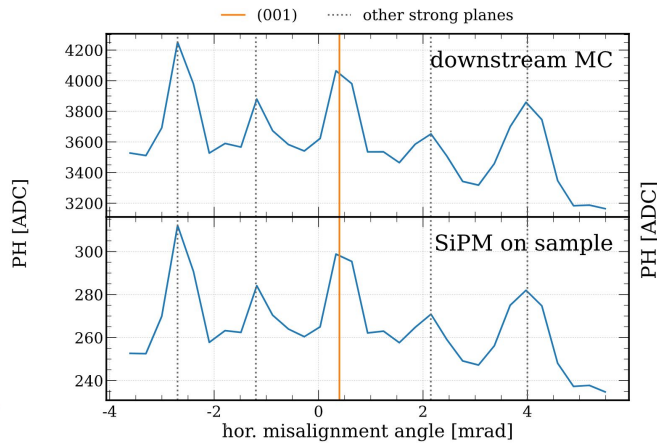
laser alignment with the particle beam reference



when mirror is aligned



when mirror is not aligned



# crystal simulation framework

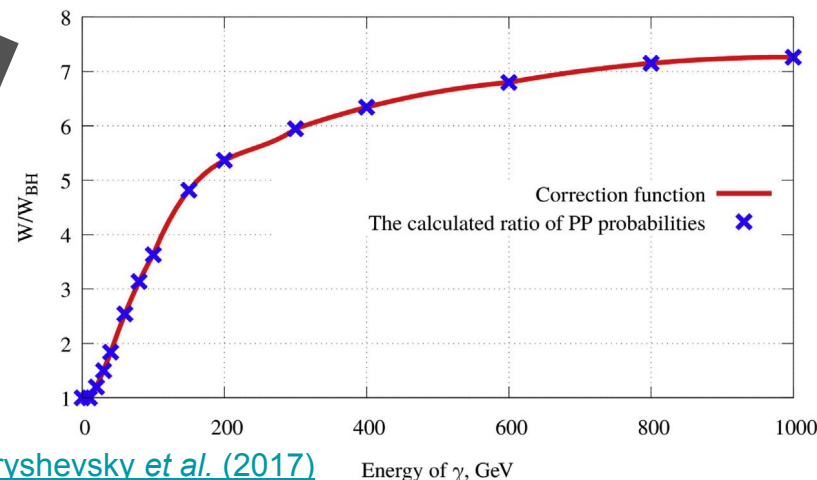
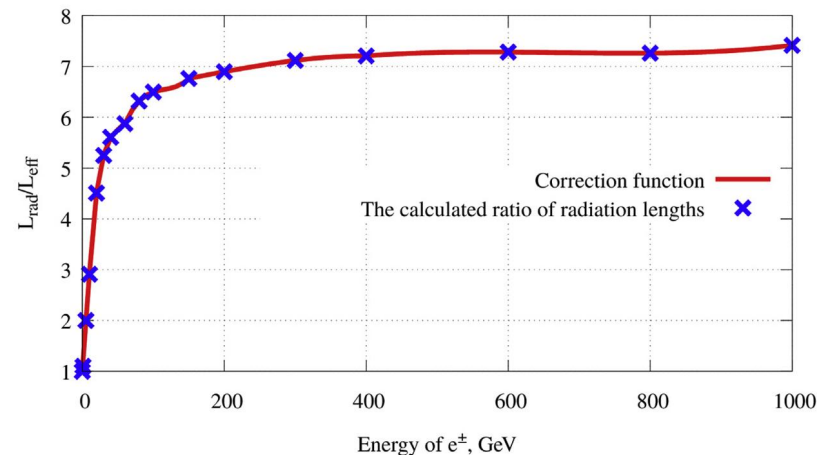
## sub- $X_0$ crystals

[Baier, Katkov & Strakhovenko \(1998\)](#) semiclassical method: simulation of the (classical) trajectories inside the crystalline lattice with (quantum) radiation emission

⇒ **Direct Integration** of the **Baier-Katkov** method implemented by INP BSU & INFN Ferrara

## multi- $X_0$ crystals

DIBK applied to thin crystal slices at different energies and angles ⇒ radiation and PP probabilities at different energies are averaged over the angles and used to rescale the Geant4 standard cross sections

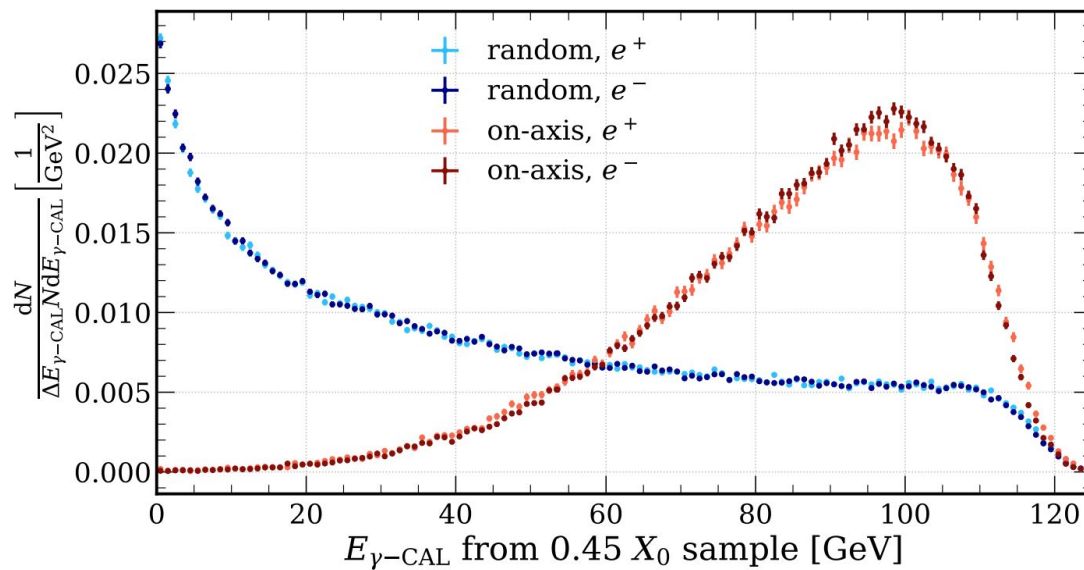


Geant4 rescaling factors for PWO 001 [Baryshevsky et al. \(2017\)](#)

Energy of  $\gamma$ , GeV

em interactions in oriented PWO

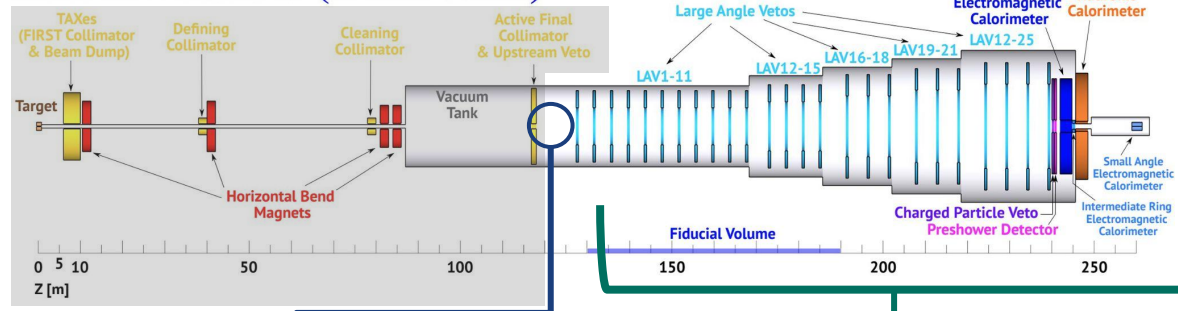
## electrons vs positrons

120 GeV/c  
electrons/positrons on

# the HIKE Small Angle Calorimeter



## HIKE Phase 3 (KLEVER)



phase 3 signal:  $K_L \rightarrow \pi^0 \nu \bar{\nu}$

i.e. two detected photons and missing momentum

main harmful background channels:

- $K_L \rightarrow \pi^0 \pi^0$  where two photons get lost
- $\Lambda \rightarrow \pi^0 n$  from upstream

**photon reconstruction is critical!**

at this point:

140 MHz (mean  $\approx 27$  GeV/c)  $K_L$   
 vs  
 440 MHz neutrons  
 198 MHz photons  $>1$  GeV  
 53 MHz photons  $>5$  GeV  
 4.1 MHz photons  $>30$  GeV

**many neutrons in the beam!**

fully hermetic, high-efficiency photon detection apparatus

along the beam path: **Small Angle Calorimeter**

- ⇒ very low photon inefficiency  $<10^{-4}$  at  $> 30$  GeV,  $<1\%$  between 5 and 30 GeV
- ⇒ insensitivity to neutrons
- ⇒ good photon/neutron disambiguation capability
- ⇒ high time resolution  $\leq 100$  ps
- ⇒ two-pulse disambiguation  $\approx$  ns
- ⇒ radiation hardness